ABSTRACT

HENNEBERRY, ALANA CARA. Effect of Musculotendon Parameter Modification on an Individualized Musculoskeletal Model. (Under the direction of Dr. Katherine Saul).

Rotator cuff tears (RCTs) are a prevalent upper limb injury, impacting more than 2 million Americans every year [1,2]. There is a gap in literature surrounding how the specific changes that define the mechanical behavior of the supraspinatus tendon because of tears impact its activation and force-generation during task performance. In this study, we aim to understand the effect of tendon mechanical parameters (*strain at one norm force*, maximum isometric force, and tendon slack length) on supraspinatus and other RC muscle-tendon forces and activations in the context of functional task performance. The overall approach was to perform a sensitivity analysis using an individualized computational upper limb model to evaluate how *strain at one norm force*, maximum isometric force, tendon slack length, and their interactions influenced rotator cuff muscle activations and muscle force. The root mean square error (RMSE) for each simulation was calculated relative to the results with the baseline model and a three-way ANOVA with interactions between *strain at one norm force,* tendon slack length, and maximum isometric force was used. Post hoc testing was performed using a one-way ANOVA without interactions for the *strain at one norm force,* tendon slack length, and maximum isometric force and Tukey Honest Significant Difference tests. The supraspinatus, infraspinatus, and subscapularis activations were all sensitive to various parameter interactions for activation and tendon force. The supraspinatus, infraspinatus, and teres minor activations showed no sensitivity to changes in the *strain at one norm force* alone. The supraspinatus activation was not sensitive to the interaction of *strain at one norm force* with maximum isometric force. All other parameters and interactions were significant for the supraspinatus, infraspinatus, and subscapularis for activation. Teres minor activation was only sensitive to tendon slack length ($p=0.01$) and the interaction of *strain at one norm force* and maximum isometric force ($p=0.04$). Supraspinatus, infraspinatus, and subscapularis tendon force were all sensitive to all parameters and their interactions ($p<0.0001$). Teres minor tendon force was not sensitive to any parameters or interactions. The supraspinatus showed the most significant effect from the parameter changes, followed by the teres minor. The tendon slack length was the most influential parameter, with all muscle activations sensitive to it for lengths 20mm and 30 mm longer than nominal. By understanding which musculotendon parameters had the greatest influence on muscle activation

levels and tendon force without confounding effects of pain or muscle atrophy, tailored studies can be conducted to develop a more comprehensive understanding of rotator cuff propagation.

Effect of Musculotendon Parameter Modification on an Individualized Musculoskeletal Model

by

Alana Cara Henneberry

A thesis submitted to the Graduate Faculty of

North Carolina State University

in partial fulfillment of the

requirements for the degree of

Master of Science

Mechanical Engineering

Raleigh, North Carolina

2025

APPROVED BY:

Dr. Katherine Saul

Chair of Advisory Committee

Dr. Jacqueline Cole

Dr. Marie Muller

Dr. Jaemin Lee

DEDICATION

To my family and friends for their unwavering love and support during the adventure that was graduate school. Without whom, I could not have made it this far.

To my mentor, Dr. Kate Saul, whose kindness, guidance, and encouragement has been so influential during this process.

BIOGRAPHY

Alana Henneberry is a second-year master's student at NC State University completing a Master of Science in Mechanical Engineering with a minor in Biomedical Engineering. Her concentration is in Biomechanical Engineering. Previously, she completed her Bachelor of Arts in Mathematics at Meredith College and her Bachelor of Science in Mechanical Engineering at NC State University in 2023 as a member of their Dual-Degree Engineering Program. While at Meredith College, she was a student-athlete with the tennis team. While on the team, she founded the campus's first student-athlete honor society. Alana graduated from the Honor's College at Meredith College with a cum laude distinction.

While at NC State University, she has focused her research on upper-limb injuries as a member of Dr. Kate Saul's Movement Biomechanics Lab (MoBL). She previously assisted with ongoing MoBL research in brachial plexus birth injury. Outside of research, Alana has worked as a course grader for Introduction to Dynamics and Dynamics of Human Movement, course teaching assistant for Mechanical Engineering Senior Design, and a course instructor for Mechanical Engineering Senior Design. She also was a camp workshop counselor for the Mechanical Engineering department summer camp for high school students. The camp was a part of a wider College of Engineering summer camp series.

In addition to research and teaching experience, Alana has industry experience from completing three consecutive engineering internships with SylvanSport in Brevard, NC. During these appointments, she worked on product development and manufacturing improvements, and technical writing for various products.

Outside of NC State, Alana is the assistant volunteer coach for the Meredith College Tennis team. Following completion of the master's program, Alana will be combining her experience from industry, collegiate athletics, and biomechanical engineering with Ping Golf where she will be a Patent Engineer within their Intellectual Property division.

ACKNOWLEDGMENTS

I would like to express my sincere gratitude to my advisor, Dr. Kate Saul, for her guidance and support over the last three years. Dr. Saul introduced me to biomechanics during my senior year of undergraduate at NC State, and her mentorship has played a key role in fueling my passion for the field. Her expertise and constructive feedback were essential in shaping the direction of this research.

I also wish to acknowledge Mason Garcia and the Nazarian Lab for their collaboration and for generously sharing their data, which significantly contributed to this study.

A special thanks to Morgan Dalman for her assistance in getting me up to speed with OpenSim. Her expertise was invaluable in helping me navigate the software.

Finally, I would like to thank my friends and family, both at NC State and afar, for their unwavering support and encouragement, and for providing moments of relief throughout this process. Their presence has made all the difference. Whether through thoughtful conversations, shared laughter, or simply being there to celebrate the milestones along the way, their support has helped keep me focused and energized. To my family, thank you for your ongoing belief in me. To my friends, thank you for sticking by my side and making this journey more enjoyable.

TABLE OF CONTENTS

LIST OF TABLES

LIST OF FIGURES

Figure 8. Boxplots of RMSE activation and tendon force levels of the teres minor with respect to (a, d) *strain at one norm force* (b, e) tendon slack length, and (c, f) maximum isometric force.

Introduction

Rotator cuff tears (RCTs) are a prevalent upper limb injury, impacting more than 2 million Americans every year [1,2]. While RCTs can be asymptomatic, symptoms of the injury include difficulty raising and lifting the arm, weakness, and pain [1–6]. The rotator cuff (RC) (Figure 1) is composed of the supraspinatus, infraspinatus, teres minor, and subscapularis [3,7–9]. The function of the rotator cuff is to stabilize the glenohumeral joint and provide force couples to keep the humeral head aligned in the glenoid of the scapula during movement [3,7,9]. When a tear occurs, the force couples become unbalanced, leading to the humeral head being less restricted and translating in the glenoid during certain movements [7,10]. In a RCT, the supraspinatus is the most commonly injured muscle [6,11,12]. According to Zhao et al., the supraspinatus is torn in 61.9% of men and 38.1% of women who experience RCTs and is the most common kind of rotator cuff tear [13]. The likelihood of RCTs increases in later adulthood, with 50% of adults aged 65 and older and 70% of adults greater than 80 years old developing supraspinatus tears [5,10,13]. Older adults are at greater risk of RCTs due to degeneration and reduced blood flow to the shoulder, which can also increase recovery time [2].

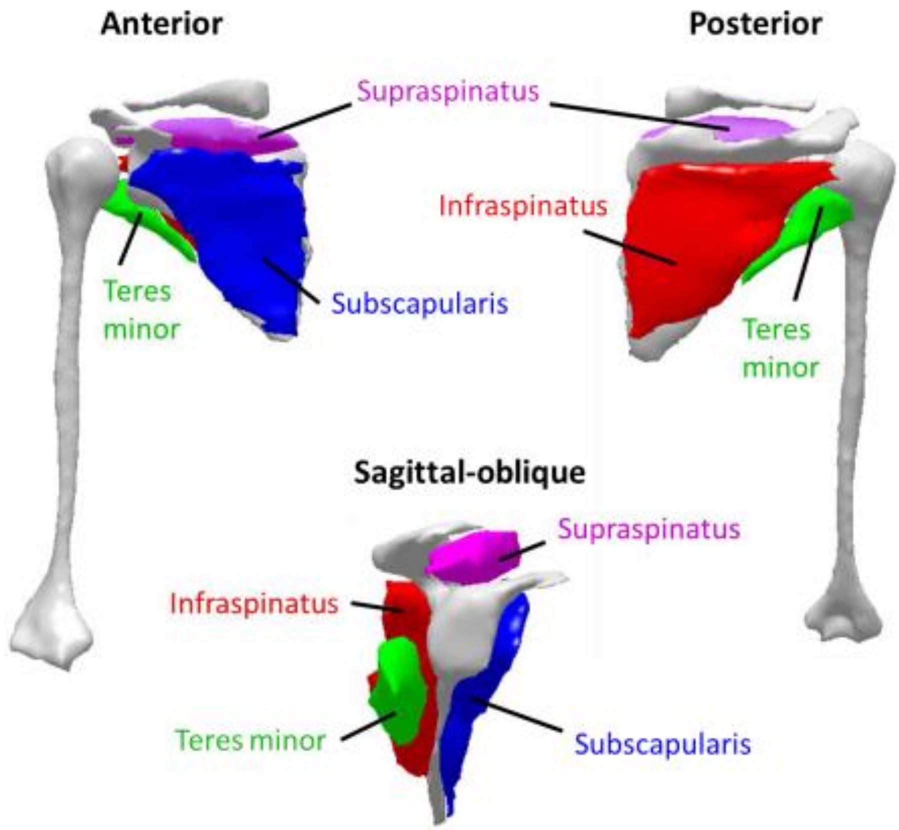

Figure 1. Rotator Cuff Muscles [14]

Tendon tears impact tendon mechanical behaviors and characteristics [9]. Collagen fibers, the primary load bearing structure of tendons, are disrupted [9,11] which contributes to reduced tendon stiffness and can reduce maximum isometric force capabilities [15]. The presence of pain symptoms has also been reportedly correlated with motion-specific decreased shoulder isometric strength [5]. Multiple sensitivity analyses in the lower limb have suggested that tendon force is more sensitive to tendon slack length changes rather than changes in muscle maximum isometric force due to muscle atrophy [16–19]; a tendon tear causes the tendon slack length to increase (Figure 2). This may be because compensation for reduced muscle volume and lower maximum isometric force may be possible via increased muscle activation [17].

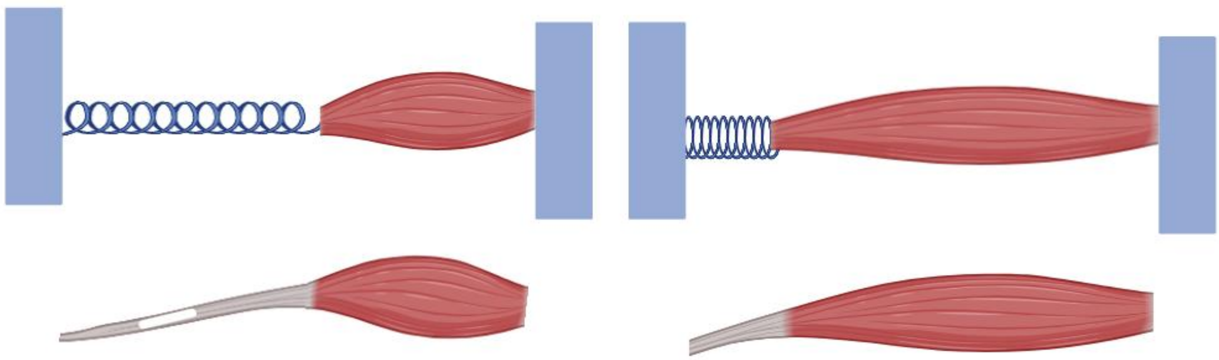

Figure 2. *Impact of tendon tears on tendon elasticity and muscle. (left) A tear to a tendon introduces a hole while elongates the tendon and reduces stiffness as represented by the stretched spring component. The muscle shortens as a result compared to a healthy, non-injured tendon (right).*

The size of the tear is another important factor in tear propagation and recovery [9,11]. RCTs are classified as partial-thickness tears or full-thickness tears, in addition to being classified based on their size. Table 1 highlights the qualifications for each tear size [3,20].

Table 1. Rotator Cuff Tear Size Measurements

Tear Size	Measurement
Small	0-1 cm
Medium	1-3 cm
Large	3-5 cm
Massive	> 5 cm

For modeling both upper- and lower-limbs, finite element analysis (FEA) and musculoskeletal software like OpenSim, Simm, and AnyBody are very popular [21]. Computational models simulate dynamic movements to study the forces and stresses experienced on anatomical points of interest. Computational and musculoskeletal modeling are popular for studies that cannot be completed in vivo. Individualizing OpenSim models by modifying anthropometric data or musculotendon parameters generates more realistic predictions of loading for specific individuals [16]. The musculotendon parameters in OpenSim 4.0 and later use the

Millard model [22], an implementation of the widely used Hill-type model of musculotendon actuators. The Hill Model has three distinct mechanical components to represent the muscle-tendon unit. The three elements are a contractile and elastic component in parallel with another elastic component (Figure 3). These represent the muscle, connective tissue, and tendon, respectively. The active contractile element is responsible for the active force production and the passive elastic element contributes to the passive force production.

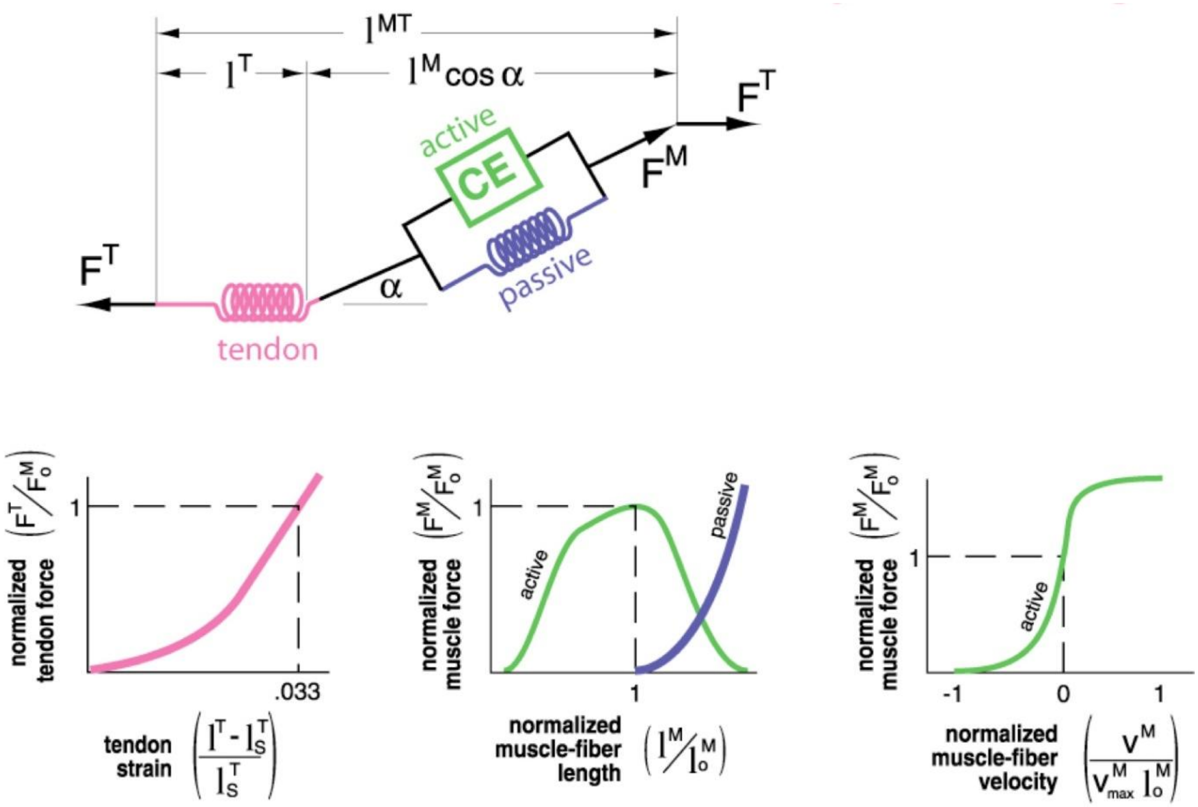

Figure 3. *Hill model (top) and graphical representations of the tendon strain on normalized muscle force (left), normalized muscle-fiber length on normalized muscle force (center), and the normalized muscle-fiber velocity on normalized muscle force (right).*

The Hill model and the Millard implementation have inherent assumptions. The classic Hill model does not represent any viscoelastic or damping properties for the tendon or parallel elastic components of the model. The active elastic component representing actin and myosin interactions does depend on shortening velocity in addition to length of the element representing the muscle fiber. (Figure 3). In addition, the Millard model includes versions with both damped elastic and rigid tendon implementations. Millard et al. provide simulation benchmarks demonstrate that the equilibrium and damped equilibrium models produce similar force profiles but have different computational speeds, and are consistent for relatively short tendons as in the rotator cuff [22]. Therefore, while velocity-dependence for contraction is captured in the model, high velocity movements that may engage the viscoelastic behavior of tendon may be less well represented than slower motions consistent with activities of daily living. The elastic tendon unit is also represented as a homogeneous material. Therefore, the Millard model cannot be modified to represent inhomogeneities because of a tear introducing spatially varying stiffnesses. OpenSim models muscles as a singular line of action representing the centroid of the muscle-tendon actuator, preventing location-dependent modifications or inhomogeneous distributions of properties within a single tendon.

With regard to the tendon portion of the Millard model (Figure 4), the overall mechanical behavior is defined by a normalized force-length curve that is parameterized using *strain at one norm force*, tendon slack length, and *stiffness at one norm force*, which are defined according to the peak isometric force of the corresponding muscle [23,24]. The *stiffness at one norm force* parameter is most directly related to measures of stiffness directly assessed in injured RCT tendon, but is a dependent parameter within the Millard model. Therefore, *strain at one norm force*, tendon slack length, and peak isometric force must be defined explicitly.

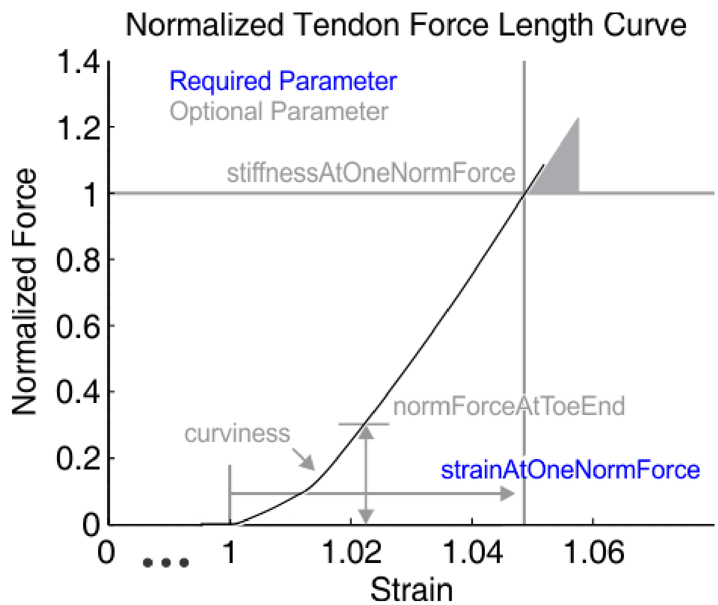

Figure 4. *Tendon Force Length Curve Utilized in OpenSim and adapted from Millard Model.*

There is a gap in literature surrounding how the specific changes that define the mechanical behavior of the supraspinatus tendon because of tears impact its activation and force-generation during task performance. To address this, we aim to perform a sensitivity analysis of tendon modeling parameters (*strain at one norm force*, maximum isometric force, and tendon slack length) on supraspinatus and other RC muscle-tendon forces and activations in the context of functional task performance. Such an analysis will enable elucidation of the roles of these isolated biomechanical tendon factors in the absence of confounding factors such as pain and muscle atrophy.

Methods

The overall approach was to use an individualized computational upper limb model to evaluate how *strain at one norm force*, maximum isometric force, tendon slack length, and their interactions influenced rotator cuff muscle activations and muscle force. All simulations were informed using previously published data of a 67 year old, right-arm dominant female with no history of rotator cuff injury [14]. The participant was recorded performing an axilla wash motion for motion capture. In the previous study by Vidt, patient information was collected including muscle volume (from medical imaging), anthropometric information, motion capture, EMG, limb strength, and a health history survey [14]. The study was approved by IRB. The axilla motion was selected for analysis here because it was identified to be significantly altered in RCT patients compared to healthy age-matched controls [14]. The axilla wash motion began with the right arm in a neutral position with the elbow extended. The participant was instructed to use this arm to touch their contralateral shoulder and then lower their arm back to the beginning position. No load was applied [14].

To create three-dimensional individualized muscle models, the muscle volume data provided in Vidt's study was used to scale the existing computational upper limb model to the individual [14,25,26]. The scaling of the model to individual muscle volumes also scaled the maximum isometric force of each muscle. This calculation was done using the following equation:

$$F = \sigma * PCSA$$

Where σ represents muscle specific tension ($50.8\ N/m^2$) and PCSA is the physiological cross-sectional area of muscle, calculated from the measured muscle volume divided by the muscle-specific optimal fiber length [26,27].

After the model was scaled, inverse kinematics was used to compute joint angles from measured marker locations recorded with motion capture cameras, and then these angles were used in a computed muscle control optimization analysis to compute muscle activations required to perform the movement task. Two versions of the model were generated using a muscle scaling optimization tool to meet the needs of the analyses. The first model had a non-fixed trunk, allowing the torso to be translated and rotated during inverse kinematics analysis to match the location of the tracking markers. The second model had a fixed trunk, prohibiting torso movement, for use during computed muscle control optimizations in order to represent the fixed torso configuration of the axilla wash task. Using previously published motion capture data, inverse kinematics for the axilla wash were computed [14]. All simulations were run with MATLAB 2021b (The Mathworks, Natick, MA) and a modified version of OpenSim 4.3 (OpenSim, Stanford University, Palo Alto, CA, version 4.3) [28]. All inverse kinematics were zero-phase filtered in MATLAB. The inverse kinematics data were used as input to the computed muscle control (CMC) tool and filtered using the default 6 Hz filter. Tracking tasks and control constraints files previously assembled by Vidt were modified and used in the setup of all CMC files. All CMC simulations employed a custom glenohumeral shoulder stability criterion in which the resulting glenohumeral contact forces were required to be directed within the envelope of the glenoid surface, as developed by McFarland et al [29].

Sensitivity Analysis. To identify the effect of each parameter on muscle activation and tendon force, a systematic series of simulations was performed using perturbations of the parameters in the nominal RCT model described above, for a total of 245 simulations (Table 2).

Table 2. Table of Nominal and All Modified Parameter Values Implemented in the Individualized Computational Models

Small Tear	Medium Tear	Large Tear	Massive Tear

Strain at One Norm Force	**Tendon Slack Length**	**Maximum Isometric Force (N)**
original = 0.03	original = 0.0395 (m)	100% = 138.54
0.05	add 2mm	90% = 124.69
0.08	add 5mm	80% = 110.84
0.09	add 7mm	70% = 96.81
0.33	add 10mm	60% = 83.13
	add 20mm	50% = 69.27
	add 30mm	40% = 55.42

The range of possible tendon slack lengths was chosen to reflect small to large rotator tuff tear sizes and retractions, as shown by the color codes in Table 2 [3]. The range of isometric forces was selected to reflect a 30% decrease in maximum isometric force due to the maximum atrophy typically reported in a full-thickness supraspinatus tear [30] while adding further reductions in force past this point. Muscle atrophy does not necessarily correspond to tear size. Therefore, maximum isometric force changes are not color coded in Table 2. The goal of simulating the reduced maximum isometric force past the point of reported full-thickness supraspinatus tears was to identify if there is a threshold beyond which mechanical stability of the glenohumeral joint is not possible. The values for *strain at one norm force* were based on normalized stiffness values for cadaveric supraspinatus muscles with and without RCT at 100N force, obtained from previously collected unpublished work by the Nazarian Lab at Beth Israel Deaconess Medical Center (courtesy Mason Garcia). After simulations were completed, the Muscle Analysis tool was used to compute muscle activations and tendon force for each simulation for the 4 muscles of the rotator cuff.

Statistical Analysis

The root mean square error (RMSE) was calculated for each simulation's activation and tendon force as compared to the nominal model. RMSE outcomes were evaluated for normality and were normally distributed. A three-way ANOVA with interactions between *strain at one norm force,* tendon slack length, and maximum isometric force was used. The significance value was set at $\alpha=0.05$. Post hoc testing was performed using one-way ANOVA with no interactions and Tukey Honest Significant Difference tests. All statistical analysis was completed using MATLAB.

Results

The supraspinatus, infraspinatus, and subscapularis were all sensitive to various parameter interactions for both activation and tendon force outcomes. The supraspinatus activation was not sensitive to *strain at one norm force* alone ($p=0.22$) or the interaction of *strain at one norm force* and maximum isometric force ($p=0.99$) (Figure 5). The supraspinatus activation was sensitive to all other parameters and their interactions ($p<0.0001$) (Figure 5). Infraspinatus activation was not sensitive to *strain at one norm force* ($p=0.14$) but was sensitive to all other parameters and their interactions ($p<0.001$) (Figure 5). Subscapularis activation was sensitive to all parameters and their interactions ($p<0.0001$) (Figure 7). Teres minor activation was only sensitive to tendon slack length ($p=0.01$) and the interaction of *strain at one norm force* and maximum isometric force ($p=0.04$) (Figure 9). Supraspinatus, infraspinatus, and subscapularis tendon force were all sensitive to all parameters and their interactions ($p<0.0001$) (Figures 4,6, and 8, respectively). Teres minor tendon force was not sensitive to any parameter nor their interactions ($p>0.05$) (Figure 10).

The Tukey-post hoc test revealed no significant differences for *strain at one norm force for activation or tendon force for any muscle,* but significant differences for both tendon slack length and maximum isometric force across activation and tendon force values depending on the muscle. Tendon slack length was associated with significant changes in activation and tendon force at 30 mm longer than nominal in the supraspinatus, infraspinatus, and subscapularis ($p<0.05$ for all) (Figures 5, 6, 7). A tendon slack length of 20 mm longer than nominal resulted in significantly different activation for supraspinatus and infraspinatus ($p<0.05$ for both) (Figures 5, 6). The teres minor tendon force did not result in any significant changes at any tendon slack length, but activation was significantly altered at tendon slack lengths that were 20 mm longer than nominal compared to nominal and 10 mm longer than nominal ($p<0.05$) (Figure 8).

RMSE for both activation and force relative to the nominal model for supraspinatus was largest for all muscles (Figure 5), followed by the teres minor (Figure 8). The RMSE values for the supraspinatus and teres minor were an order of magnitude larger than the infraspinatus and subscapularis (Figure 5, 6, 7, respectively). The infraspinatus and subscapularis were most sensitive to supraspinatus maximum isometric force (Figure 6, 7). Simulations with the longest tendon slack length (30 mm longer than nominal) increased RMSE values for activation and tendon force for the supraspinatus (Figure 5), infraspinatus (Figure 6) and subscapularis (Figure 7). Instances of RMSE outliers in the figures arose from interactions with other parameters as described in the relevant statistical reports.

When the tendon slack length was 30 mm longer than nominal, the supraspinatus was unable to compensate for the reduced force-generating capacity. This was evident from initially saturated activations of 1.0 at early stages of the task movement, and then activation levels near zero for the remainder of the movement; in the nominal and other solutions, the muscle was activated throughout the motion. The infraspinatus, subscapularis, and teres minor continued to be activated during the whole motion to achieve the desired kinematics, without contributions from supraspinatus in these cases.

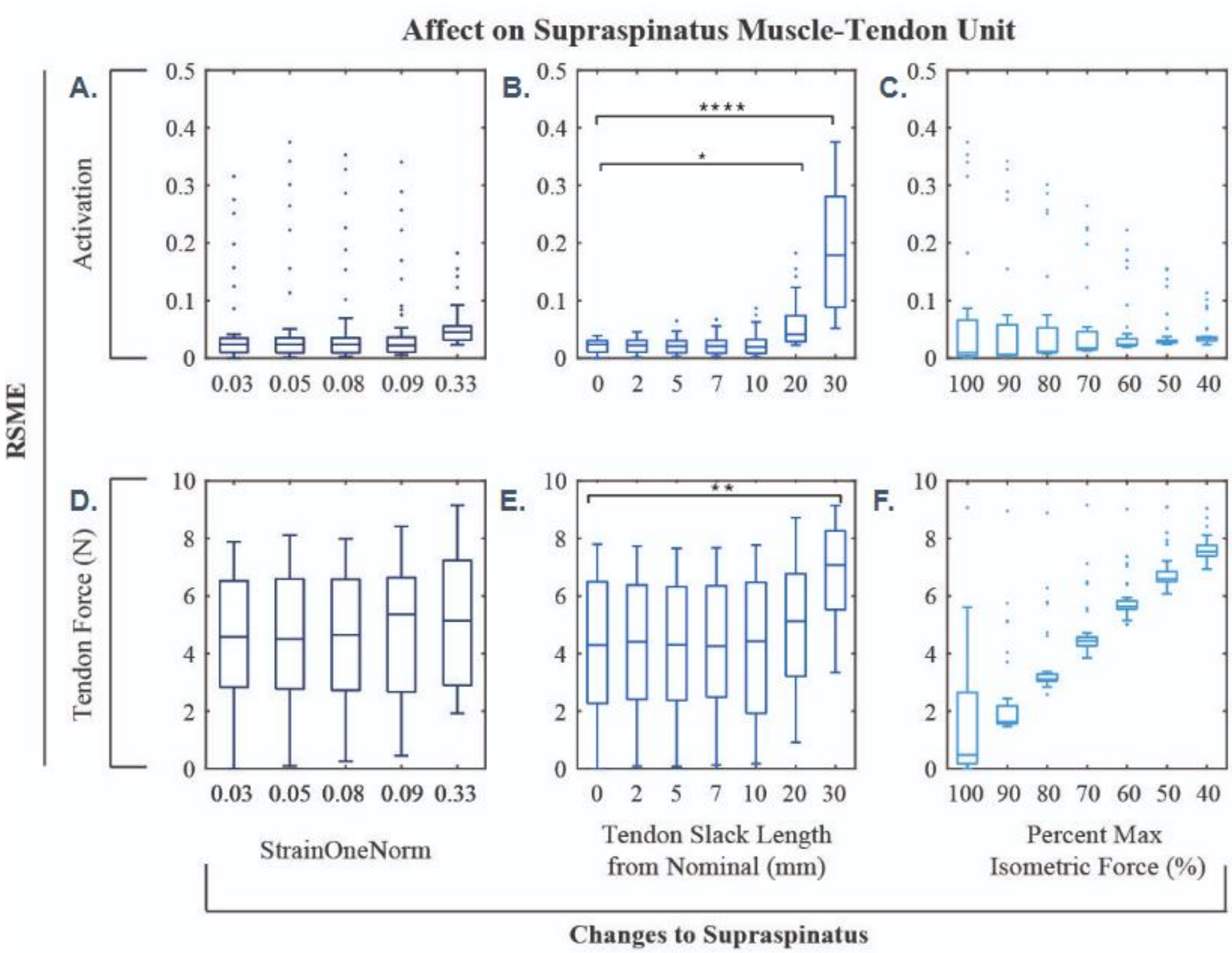

Figure 5. *RMSE activation and tendon force values of the supraspinatus with respect to (a, d) strain at one norm force, (b, e) tendon slack length, and (c, f) maximum isometric force. Due to the scale of activation levels being 0-1, the RMSE values were all low but had several outliers. The outliers (a-c) are all associated with interactions with tendon slack lengths of 20 mm longer than nominal or 30 mm longer than nominal varying across (a) strain at one norm force and (c) maximum isometric force values. (a) The average RMSE ranges from* 4.52×10^{-2} *(*$\pm 7.17 \times 10^{-2}$*) to* 5.39×10^{-2} *(*$\pm 3.4 \times 10^{-2}$*) as strain increases from 0.033 to 0.33, respectively. (b) The average RMSE ranges from* 2.07×10^{-2} *(*$\pm 1.22 \times 10^{-2}$*) to* 0.19 *(*± 0.11*) as tendon slack length increases from nominal to 30 mm longer than nominal. (c) The average*

RMSE ranges from 4.09×10^{-2} *(*$\pm 2.18 \times 10^{-2}$*) to* 6.48×10^{-2} *(*± 0.11*) as the maximum isometric force increases from 40% to 100%. (d) The average RMSE was roughly* 4.5 ± 2.45 *N until a strain of 0.33 when the average RMSE increased to* 5.29 ± 2.37 *N. (e) The average RMSE stayed around* 4.19 ± 2.4 *N until a length of 20 mm longer than nominal and 30 mm longer than nominal when it increased to* 4.8 ± 2.3 *N and* 6.7 ± 1.8 *N, respectively. (f) The average RMSE for maximum isometric force varied from* 7.64 ± 0.42 *N at 40% to* 1.51 ± 2.03 *N. The outliers are all associated with interactions with larger tendon slack lengths of 30 mm longer than nominal and occasionally 20 mm longer than nominal. (b, e) There was a significant difference in activation and tendon force when the tendon slack length was increased by 30 mm compared to the nominal. The activation also was significantly difference with a 20 mm tendon slack length addition.*

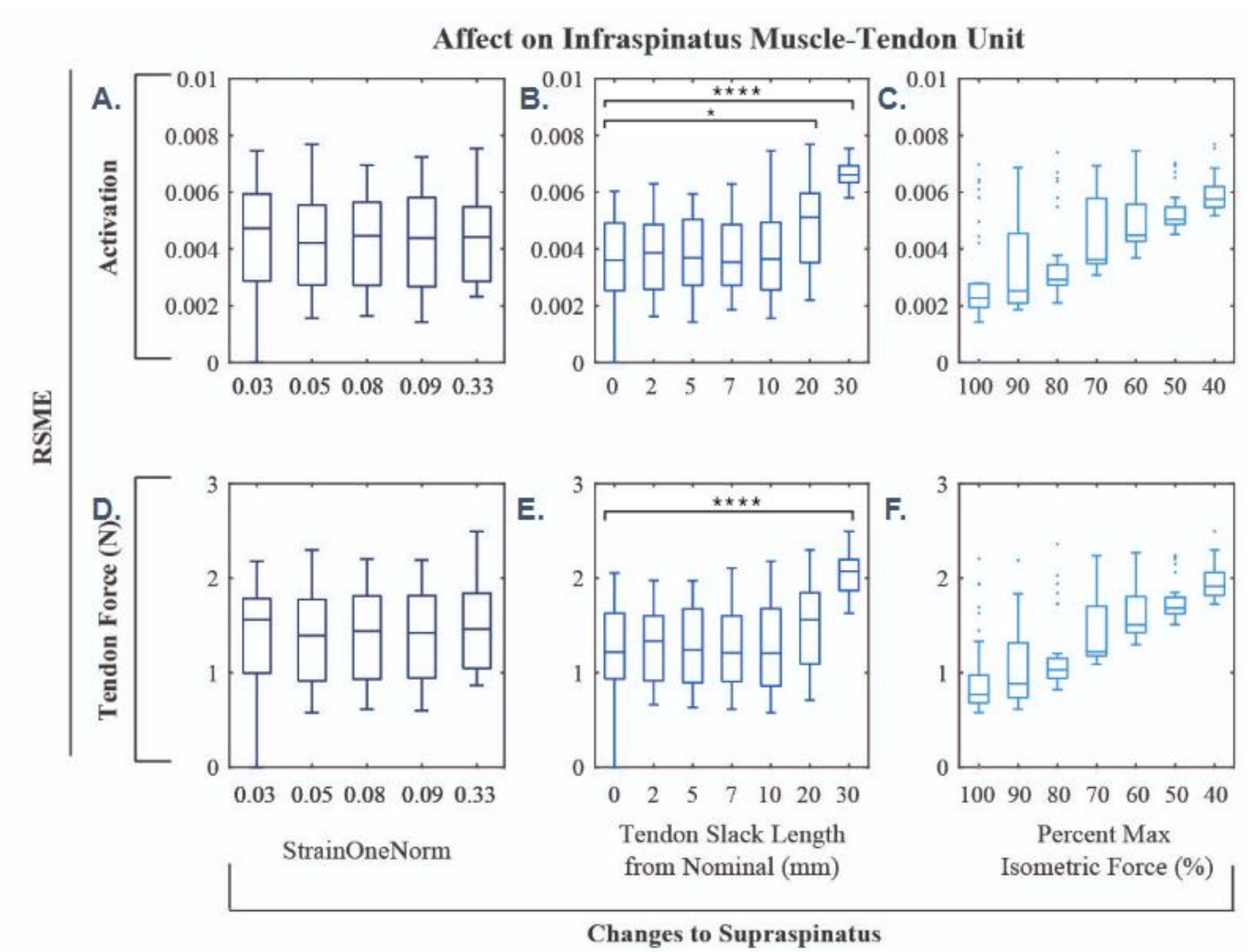

Figure 6. *RMSE tendon force values of the infraspinatus with respect to changes in supraspinatus (a, d) strain at one norm force (b, e) tendon slack length, and (c. f) maximum isometric force. (a) The average RMSE activation is around* 4.5×10^{-3} *(*$\pm 1.6 \times 10^{-3}$) *. (b) The average RMSE activation is* 3.8×10^{-3} *(*$\pm 1.4 \times 10^{-3}$) *for smaller tendon slack lengths (<0.0595m). At 0.0595m, the average RMSE increases to* 4.8×10^{-3} *(*$\pm 1.5 \times 10^{-3}$)*, and then increases again to* 6.6×10^{-3} *(*$\pm 4.0 \times 10^{-4}$) *at 30 mm longer than nominal. (c) The average RMSE value differs with each magnitude of force and ranges from* 5.9×10^{-3} *(*$\pm 6.0 \times 10^{-4}$) *to* 2.9×10^{-3} *(*$\pm 1.7 \times 10^{-3}$) *and 40% and 100%, respectively. The outliers come from being paired with a larger tendon slack length of 20 mm longer than nominal or 30 mm longer than nominal. At 100%, there were two outliers that came from 2 mm longer and 10 mm longer than nominal. (d) The average RMSE value stays relatively constant across all strain values. The minimum average occurs at 0.0502 and is* 1.37 ± 0.48 *N while the maximum average is at 0.33 and is* 1.49 ± 0.47 *N. (e) The average RMSE value stays relatively constant around* 1.26 ± 0.42 *N while the tendon slack length is between nominal and 10 mm longer than nominal. At 10 mm longer than nominal, the average increases to* 1.51 ± 0.47 *N and then again to* 2.02 ± 0.21 *N at 30 mm longer than nominal. (f) The average RMSE value varies from 40% to 100% at* 1.95 ± 0.17 *N to* 0.94 ± 0.46 *N. The outliers all come from interactions with tendon slack lengths of 20 mm or 30 mm longer than nominal.*

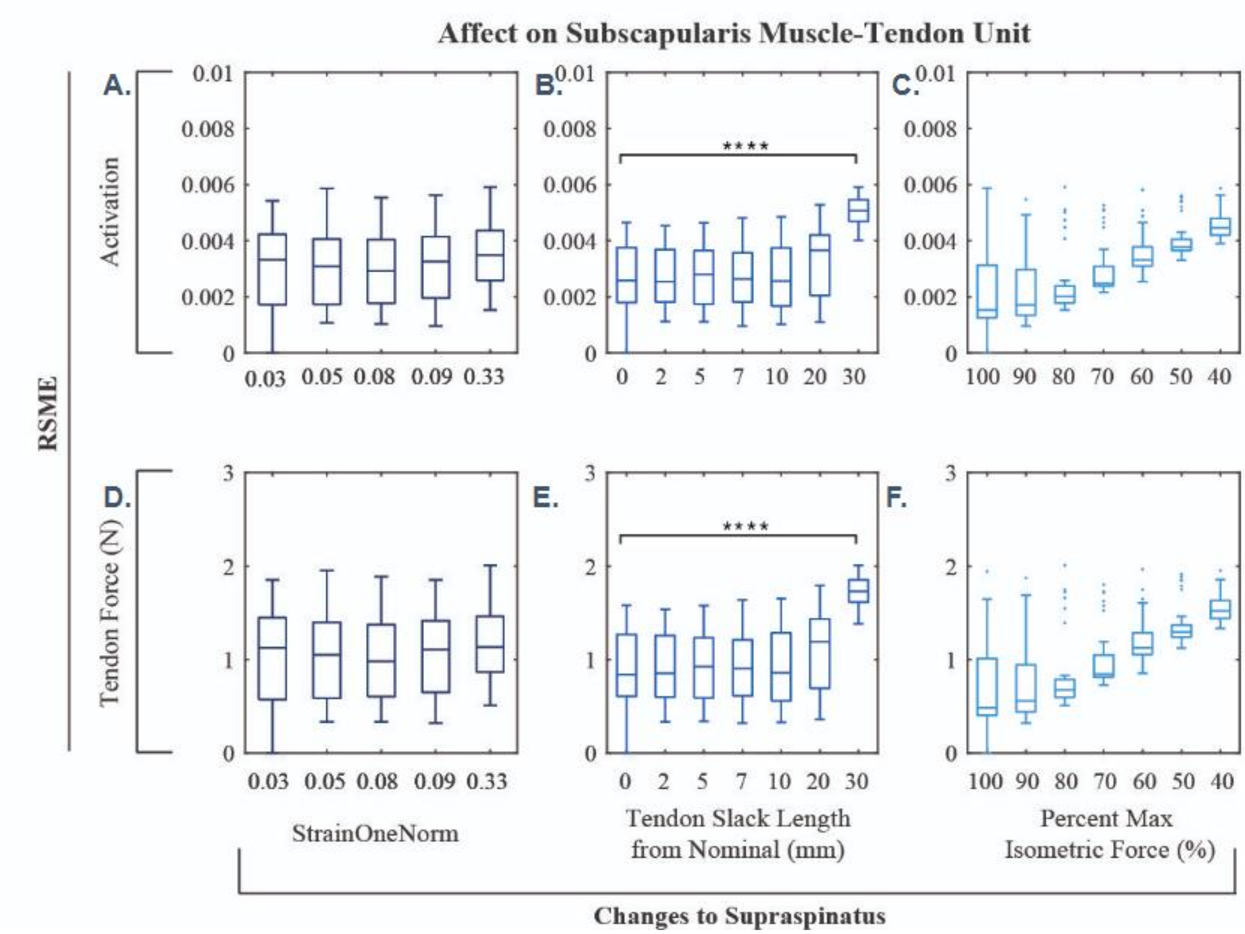
Affect on Subscapularis Muscle-Tendon Unit
RSME
A.
B.
C.
D.
E.
F.
Activation
Tendon Force (N)
0.01
0.008
0.006
0.004
0.002
0
3
2
1
0
****
0.03 0.05 0.08 0.09 0.33
0 2 5 7 10 20 30
100 90 80 70 60 50 40
StrainOneNorm
Tendon Slack Length from Nominal (mm)
Percent Max Isometric Force (%)
Changes to Supraspinatus

Figure 7. *RMSE tendon force values of the subscapularis with respect to changes in supraspinatus (a, d) strain at one norm force (b, e) tendon slack length, and (c, f) maximum isometric force. (a) The average RMSE showed little variation between strain values and ranged between* 3.0×10^{-3} *(*$\pm 1.4 \times 10^{-3}$) *and* 3.6×10^{-3} *(*$\pm 1.2 \times 10^{-3}$). *(b) The average RMSE stayed around* 2.8×10^{-3} *(*$\pm 1.1 \times 10^{-3}$) *for tendon slack lengths from nominal to 10 mm longer. The average RMSE increased to* 3.2×10^{-3} *(*$\pm 1.3 \times 10^{-3}$) *and* 5.0×10^{-3} *(*$\pm 5.0 \times 10^{-4}$) *at 20 mm and 30 mm longer than nominal, respectively. (c) The average RMSE value ranged from* 4.6×10^{-3} *(*$\pm 5.0 \times 10^{-4}$) *to* 2.2×10^{-3} *(*$\pm 1.4 \times 10^{-3}$) *as maximum isometric force increased from 40% to 100%. (d) The average RMSE value showed little variation across strain values and ranged from* 1.0 ± 0.44 *N and* 1.2 ± 0.40 *N. Similarly, the RMSE values for tendon slack length (e) ranged showed minimal variation from nominal to 10 mm longer than nominal with averages around* 0.93 ± 0.38 *N. At 20 mm longer than nominal, the average increased to* 1.08 ± 0.43 *N and then* 1.72 ± 0.17 *N at 0.30 mm longer. (f) The average RMSE showed greater variation with maximum isometric force than with strain at one norm force or tendon slack length. At 40%, the average RMSE was* 1.55 ± 0.15 *N. The average decreased to* 0.71 ± 0.45 *N at 100%. The outliers all come from interactions with a tendon slack length of 20 mm or 30 mm longer than nominal.*

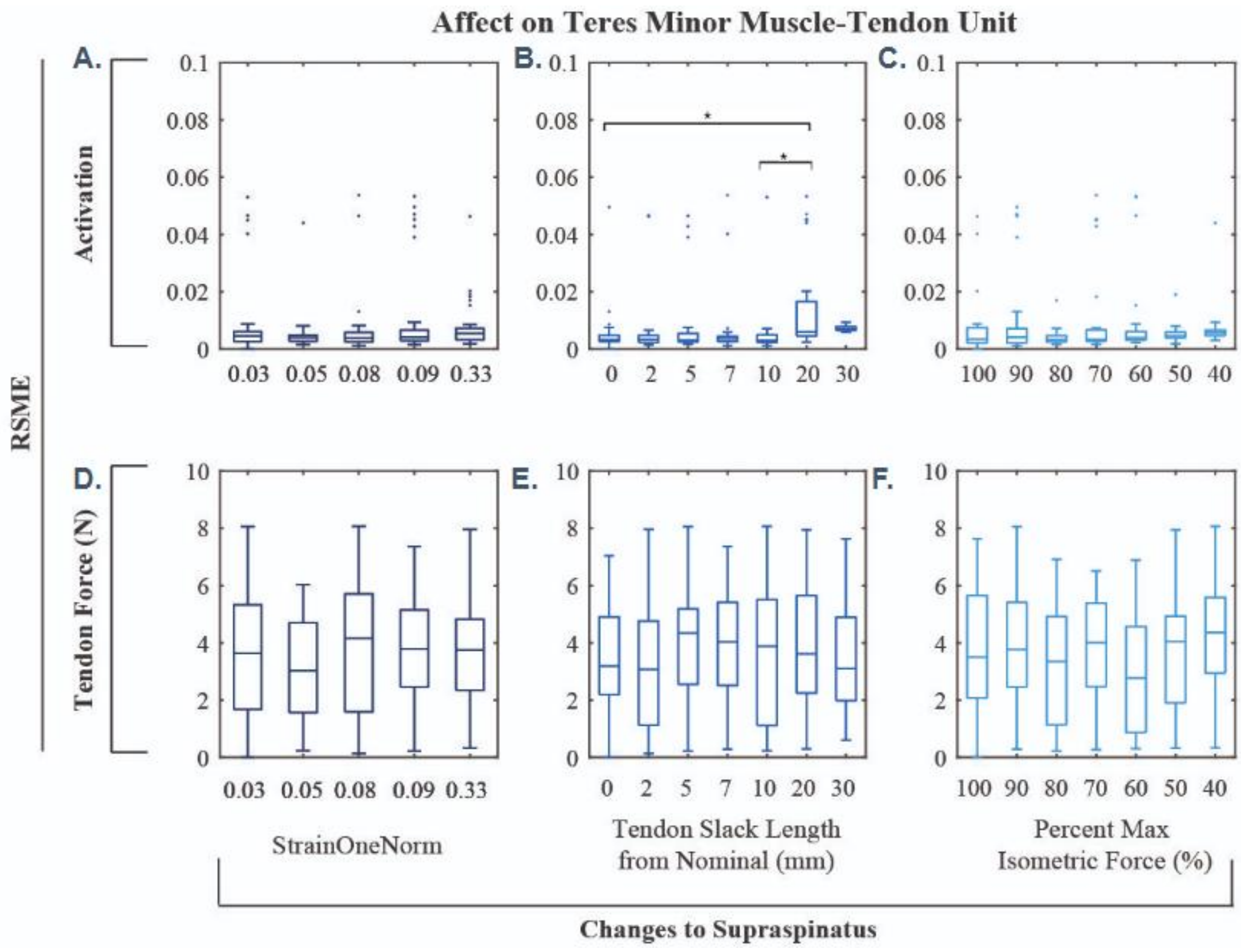

Affect on Teres Minor Muscle-Tendon Unit
A.
B.
C.
RSME
Activation
0.1
0.08
0.06
0.04
0.02
0
0.03 0.05 0.08 0.09 0.33
0 2 5 7 10 20 30
100 90 80 70 60 50 40
D.
E.
F.
Tendon Force (N)
10
8
6
4
2
0
StrainOneNorm
Tendon Slack Length from Nominal (mm)
Percent Max Isometric Force (%)
Changes to Supraspinatus

Figure 8. *RMSE activation and tendon force values of the teres minor with respect to changes in supraspinatus (a, d) strain at one norm force (b, e) tendon slack length, and (c, f) maximum isometric force. (a) The RMSE of activation levels varied from* 4.9×10^{-3} *(*$\pm 6.0 \times 10^{-3}$*) at 0.0502, to* 9.3×10^{-3}*(*$\pm 1.4 \times 10^{-2}$*) at 0.0947. The outliers came from interactions with a variety of tendon slack length and maximum isometric force. (b) The average RMSE was a minimum at 10 mm longer than nominal with an average of* 4.9×10^{-3}*(*$\pm 8.5 \times 10^{-3}$*). The average RMSE was a maximum at 20 mm longer than nominal with an average of* 1.2×10^{-2}*(*$\pm 1.4 \times 10^{-2}$*). The outliers varied across strain at one norm force and maximum isometric force. (c) The average RMSE was the least at 80% with an average of* 4.0×10^{-3}*(*$\pm 2.7 \times 10^{-3}$*). The average reached a maximum at 70% with an average of* 9.1×10^{-3}*(*$\pm 1.4 \times 10^{-3}$*). The outliers come predominantly from interaction with a tendon slack length of 20 mm longer than nominal, though smaller lengths are also present when paired with high strain values. (d) The average RMSE stays between 3-4 N, with an average of* 3.73 ± 1.98 *N. (e) The average RMSE also stayed between 3-4 N with an average of* 3.41 ± 1.89 *N. (f) The average RMSE showed more variation than strain at one norm force or tendon slack length. The minimum average RMSE for occurred at 60% with an average of* 2.91 ± 2.06 *N and reached a maximum at 40% with an average of* 4.23 ± 1.95 *N.*

Discussion

This study aimed to determine which musculotendon parameters had the greatest impact on RC muscle activation and tendon force, and which muscles were most affected. This information could form the basis for future studies to explore neuromuscular compensations from rotator cuff tears in more detail. By understanding which musculotendon parameters had the greatest influence on muscle activation levels and tendon force without confounding effects of pain or muscle atrophy, tailored studies can be conducted to develop a more comprehensive understanding of rotator cuff tear propagation. Consistent with previous studies on upper and lower limbs, this study indicated that the rotator cuff muscles were impacted in activation and tendon force due to changes in the *strain at one norm force* [23], tendon slack length [16–19,23,31], and maximum isometric force [17]. Post-hoc significance testing indicated that activation and tendon force were more sensitive to increased tendon slack length than maximum isometric force or *strain at one norm force*. This is consistent with other studies indicating that tendon force is more sensitive toto tendon slack length than to changes in maximum isometric force in both upper- and lower-limb studies [16–19].

When tendon slack length is increased or maximum isometric force is decreased, the supraspinatus force-generating capacity is naturally reduced according to the force-length relationship governing muscle force production. Consequently, there was a greater difference in the activation and tendon force produced by the supraspinatus than the other muscles. This is consistent with other studies which show reduced force production [15,17] and higher activation as a result of an rotator cuff tear [32,33]. For most parameter combinations, the supraspinatus was able to increase activation adequately to compensate for the reduced force-generating capacity, leading to limited changes in other muscles. However, for larger increases in tendon slack length, activation could not adequately compensate, and other muscle contributions were altered as well to maintain the overall kinematic requirements of the task.

The tendon slack lengths representing medium to large tears (20 mm and 30 mm longer than nominal) resulted in greater RMSE for activation and tendon force for the supraspinatus, infraspinatus, and subscapularis (Figures 5-7). This would imply that when the supraspinatus is weaker, the infraspinatus and subscapularis are recruited to a greater extent compensate. A tear of 3cm (30 mm longer than nominal) causes similar RMSE for muscle activation in infraspinatus and supraspinatus as compared to simulations with maximum isometric supraspinatus force that is 40% nominal. This is consistent with previous findings that showed simulations modifying upper- or lower-limb muscle-tendon parameters while individualizing OpenSim models were more sensitive to changes in tendon slack length than maximum isometric force [16–19].

While the supraspinatus tendon force varied from an average RMSE of 7.64 ± 0.42 N at 40% to 1.51 ± 2.03 N at 100% of supraspinatus maximum isometric force, the teres minor had smaller change with altered supraspinatus maximum isometric force, from RMSE of 2.91 ± 2.06 N at 60% to 4.23 ± 1.95N at 40%. The infraspinatus and subscapularis never reached an average RMSE as high of 2.91 N, but showed variability in RMSE values in response to greater simulated tears. This indicates that the tendon force was significantly impacted by the severity of tears simulated. While the teres minor showed higher RMSE values than the infraspinatus and subscapularis, the teres minor RMSE values were more stable across trials. This indicates the variability of tear severity was less significant, but rather any change to the model caused a larger RMSE. Teres minor tendon force was slightly reduced relative to the nominal model. Previous studies simulating the effect of rotator cuff tear severity on muscle forces during the axilla wash suggest that the teres minor will increase force contribution in the presence of an injured supraspinatus as tear severity advances [34]. However, the Pataky et al. study examines tear effects that were far larger than simulated here, with the minimum atrophy represented being 50% loss of maximum isometric force of just the supraspinatus. The Pataky study progressively increased tear severity by reducing supraspinatus maximum isometric force until a severe, three-tendon tear was represented by 0% of the supraspinatus maximum isometric force with 25% of the infraspinatus and subscapularis maximum isometric force. If our study were continued in the future to explore more extensive tears, including tears of other rotator cuff muscles, the teres minor may show a compensatory increase in tendon force production once the infraspinatus or subscapularis muscles force capabilities are reduced.

The assumptions introduced with the Hill and Millard model likely do not significantly impact the results. Dynamic effects of the motion were likely minimal. For example, the active force production already accounts for the shortening velocity of the muscle-fiber (Figure 3) and the chosen task was sufficiently slow that any viscoelastic effects on the tendon were not relevant. OpenSim models the muscles as a simplified line of action that does not allow for spatial specifications of muscle-tendon parameters. Assumptions of spatial homogeneity in the model representation are unlikely to affect overall estimates of force and activation arising from the lumped parameter model. The specific model parameters directly represent muscle retraction (tendon slack length) and effective stiffness (*strain at one norm force*) that have been measured clinically or experimentally. However, there are observed spatial differences in stiffness throughout the tendon depending on the location, geometry, and orientation of the tear [9,11]. Consequently, a method that captures this inhomogeneity may provide greater insight into the tear properties itself, as well as the propagation of the tear. Finite element modeling of the 3D characteristics of the tear geometry and tendon tissue from medical imaging may provide greater spatial information regarding tendon tear behavior. However, the implementation of the Hill-type model within a dynamic system, as in OpenSim, allows for simulation of a full dynamic task and predictions of muscle excitations coordinated across multiple muscle-tendon elements, which is typically not possible with finite element implementations that allow for incorporation of more complex and inhomogeneous spatial and viscoelastic properties. Thus, different models are appropriate alone and in combination depending on the scientific question.

The aim of the current study was to identify the parameters that are most influential and warrant future examination as either variables or boundary conditions for future experimental or computational approaches. Consequently, these assumptions do not compromise the primary objective.

There were additional limitations of the study design. The sensitivity analyses were based on a single nominal baseline simulation developed from one individual and one motion. This decision was made to isolate the effects of individual parameters without the confounding effects of kinematic and anatomical variability. This study was designed to evaluate which parameters were most sensitive and warrant future investigation. Future work will incorporate a wider variety of model configurations designed to represent a broader range of age, sex, functional mobility of the upper arm, and task requirements. A formal stochastic approach (e.g. Monte Carlo) would also refine parameter selection to allow random selection from a distribution of parameters as opposed to discrete parameter values. The current study performed perturbations among all independent variable values to form an understanding of how the relationship between the values impact tendon force production and activation. However, an injury would not have a typical *strain at one norm force* of 0.033 and maximum isometric force of 100% but a 30 mm increase in tendon slack length. Therefore, covariance between parameters can be incorporated, such as *strain at one norm force* and tendon slack length, so that each simulation was a more accurate depiction of an injured muscle-tendon unit. Future work may also explore sensitivity to muscle parameter changes associated with RCT, such as muscle shortening due to retraction.

The results of this study highlight the importance of future studies on the modification and individualization of musculotendon parameters in musculoskeletal modeling of pathologies. There is significant room for expanding this research to identify the absolute mechanical limitations of the rotator cuff because of a supraspinatus tear. Further studies including simulated tears to the other rotator cuff tears would also elicit insightful information on how the rotator cuff behaves when multiple sources of weakness are introduced. Additionally, iterative modeling with integrated finite element analysis to simulate tear propagation from continued stress or strain on a torn rotator cuff could grant insights into the limitations of the muscle tissue and tear propagation. Similar studies have been previously published for prediction of bone formation for brachial plexus birth injury [35]. Implementing modifications to the geometry of the glenohumeral joint bones in simulations to represent individualized anatomy (e.g., bone spurs, fractures, etc.) would likely impact muscle force if appropriate to capture concomitant injuries. While other studies have examined the effect of modifications of musculotendon parameters on force or activation, this specific set of independent variables has not been studied together in simulating a supraspinatus injury, to the best of my knowledge. As such, the result of this study uniquely provides insight into how shoulder function and muscle coordination will respond to these simulated supraspinatus tears and allows more informed predictions about anticipated outcomes of RCT.

Conclusion

The goal of this study was to determine the effects of altering various parameters of the supraspinatus muscle on the activation and tendon force of the four rotator cuff muscles. In analyzing the results of this study, the *strain at one norm force*, maximum isometric force, and tendon slack length were all collectively adjusted. The supraspinatus, infraspinatus, and subscapularis were all sensitive to parameter interactions for activation and tendon force. Muscle activation and tendon force were most sensitive to tendon slack length and maximum isometric force. The teres minor activation and tendon force demonstrated the least sensitivity to changes of supraspinatus parameters.

While this study revealed that outcomes were sensitive to musculotendon parameters in an individualized model, future studies should be conducted to explore the effects on the three-dimensional geometry of a tear. Future studies should also be conducted to extend this work to simulate tears to multiple RC muscles. Once there is greater understanding about which mechanical components of a tear impact reduced force production or ability to complete tasks of daily living, clinicians can make more educated decisions during the diagnostic process. This knowledge can also identify the populations most at risk for tear or continued tear propagation. Once a deeper understanding of rotator cuff tears and their progression is established, medical and physical therapy interventions can be fine-tuned to promote improved recovery and reduce the worsening of the injury.

References

[1] 2023, “Rotator Cuff,” Clevel. Clin. [Online]. Available: https://my.clevelandclinic.org/health/body/rotator-cuff. [Accessed: 25-Jan-2025].

[2] “Rotator Cuff Tear,” Clevel. Clin. [Online]. Available: https://my.clevelandclinic.org/health/diseases/8291-rotator-cuff-tear.

[3] William Levine MD, 2025, “Rotator Cuff Tears,” Rotator Cuff Tears OrthoBullets. [Online]. Available: https://www.orthobullets.com/shoulder-and-elbow/3043/rotator-cuff-tears. [Accessed: 25-Jan-2025].

[4] “Partial Rotator Cuff Tear,” Johns Hopkins Med. [Online]. Available: https://www.hopkinsmedicine.org/health/conditions-and-diseases/partial-rotator-cuff-tear. [Accessed: 25-Jan-2025].

[5] Ueda, Y., Tanaka, H., Tomita, K., Tachibana, T., Inui, H., Nobuhara, K., Umehara, J., and Ichihashi, N., 2020, “Comparison of Shoulder Muscle Strength, Cross-Sectional Area, Acromiohumeral Distance, and Thickness of the Supraspinatus Tendon between Symptomatic and Asymptomatic Patients with Rotator Cuff Tears,” J. Shoulder Elbow Surg., **29**(10), pp. 2043–2050. https://doi.org/10.1016/j.jse.2020.02.017.

[6] Miller, J. E., Higgins, L. D., Dong, Y., Collins, J. E., Bean, J. F., Seitz, A. L., Katz, J. N., and Jain, N. B., 2016, “Association of Strength Measurement with Rotator Cuff Tear in Patients with Shoulder Pain: The Rotator Cuff Outcomes Workgroup Study,” Am. J. Phys. Med. Rehabil., **95**(1), pp. 47–56. https://doi.org/10.1097/PHM.0000000000000329.

[7] Asghar, A., Ghosh, S., and Narayan, R., 2020, “Revisiting the Anatomy of Rotator Cuff Relevant to Rotator Cuff Injury,” Natl. J. Clin. Anat., **9**(1), p. 1. https://doi.org/10.1055/s-0040-1709029.

[8] Matthewson, G., Beach, C. J., Nelson, A. A., Woodmass, J. M., Ono, Y., Boorman, R. S., Lo, I. K. Y., and Thornton, G. M., 2015, “Partial Thickness Rotator Cuff Tears: Current Concepts,” Adv. Orthop., **2015**, pp. 1–11. https://doi.org/10.1155/2015/458786.

[9] Garcia, M., Landi, G., Covan, B., Caro, D., Khak, M., Razavi, A. H., DeAngelis, J. P., Ramappa, A. J., and Nazarian, A., 2024, “Effect of Tear Size and Location on Supraspinatus Tendon Strain During Activities of Daily Living and Physiotherapy,” Ann. Biomed. Eng., **52**(9), pp. 2496–2508. https://doi.org/10.1007/s10439-024-03538-5.

[10] Mattar, L. T., Popchak, A. J., Anderst, W. J., Musahl, V., Irrgang, J. J., and Debski, R. E., 2022, “Associations between Range of Motion, Strength, Tear Size, Patient-Reported Outcomes, and Glenohumeral Kinematics in Individuals with Symptomatic Isolated Supraspinatus Tears,” J. Shoulder Elbow Surg., **31**(6), pp. 1261–1271. https://doi.org/10.1016/j.jse.2021.12.032.

[11] Thunes, J., Matthew Miller, R., Pal, S., Damle, S., Debski, R. E., and Maiti, S., 2015, “The Effect of Size and Location of Tears in the Supraspinatus Tendon on Potential Tear Propagation,” J. Biomech. Eng., **137**(8), p. 081012. https://doi.org/10.1115/1.4030745.

[12] Santos, I., Pichler, L., Saller, M. M., Thorwächter, C., Müller, J. G., Traxler, H., Pietschmann, M. F., Tauber, M., and Müller, P. E., 2023, “Effect of Shape and Size of Supraspinatus Tears on Rotator Cuff Strain Distribution: An in Vitro Study,” J. Shoulder Elbow Surg., **32**(2), pp. e71–e83. https://doi.org/10.1016/j.jse.2022.08.023.

[13] Zhao, J., Luo, M., Liang, G., Wu, M., Pan, J., Zeng, L., Yang, W., and Liu, J., 2021, “Risk Factors for Supraspinatus Tears: A Meta-Analysis of Observational Studies,” Orthop. J. Sports Med., **9**(10), p. 23259671211042826. https://doi.org/10.1177/23259671211042826.

[14] Vidt, M. E., Santago, A. C., Marsh, A. P., Hegedus, E. J., Tuohy, C. J., Poehling, G. G., Freehill, M. T., Miller, M. E., and Saul, K. R., 2018, "Modeling a Rotator Cuff Tear: Individualized Shoulder Muscle Forces Influence Glenohumeral Joint Contact Force Predictions," Clin. Biomech., **60**, pp. 20–29. https://doi.org/10.1016/j.clinbiomech.2018.10.004.

[15] Brumitt, J., and Cuddeford, T., 2015, "CURRENT CONCEPTS OF MUSCLE AND TENDON ADAPTATION TO STRENGTH AND CONDITIONING," Int. J. Sports Phys. Ther., **10**(6), pp. 748–759.

[16] Arslan, Y. Z., and Karabulut, D., 2021, "SENSITIVITY OF MODEL-PREDICTED MUSCLE FORCES OF PATIENTS WITH CEREBRAL PALSY TO VARIATIONS IN MUSCLE-TENDON PARAMETERS," J. Mech. Med. Biol., **21**(01), p. 2150008. https://doi.org/10.1142/S0219519421500081.

[17] Diaz, M. T., Harley, J. B., and Nichols, J. A., 2024, "Sensitivity Analysis of Upper Limb Musculoskeletal Models During Isometric and Isokinetic Tasks," J. Biomech. Eng., **146**(2), p. 021005. https://doi.org/10.1115/1.4064056.

[18] Ackland, D. C., Lin, Y.-C., and Pandy, M. G., 2012, "Sensitivity of Model Predictions of Muscle Function to Changes in Moment Arms and Muscle–Tendon Properties: A Monte-Carlo Analysis," J. Biomech., **45**(8), pp. 1463–1471. https://doi.org/10.1016/j.jbiomech.2012.02.023.

[19] De Groote, F., Van Campen, A., Jonkers, I., and De Schutter, J., 2010, "Sensitivity of Dynamic Simulations of Gait and Dynamometer Experiments to Hill Muscle Model Parameters of Knee Flexors and Extensors," J. Biomech., **43**(10), pp. 1876–1883. https://doi.org/10.1016/j.jbiomech.2010.03.022.

[20] Rashid, M. S., Cooper, C., Cook, J., Cooper, D., Dakin, S. G., Snelling, S., and Carr, A. J., 2017, "Increasing Age and Tear Size Reduce Rotator Cuff Repair Healing Rate at 1 Year: Data from a Large Randomized Controlled Trial," Acta Orthop., **88**(6), pp. 606–611. https://doi.org/10.1080/17453674.2017.1370844.

[21] Farshidfar, S. S., Cadman, J., Deng, D., Appleyard, R., and Dabirrahmani, D., 2022, "The Effect of Modelling Parameters in the Development and Validation of Knee Joint Models on Ligament Mechanics: A Systematic Review," PLOS ONE, **17**(1), p. e0262684. https://doi.org/10.1371/journal.pone.0262684.

[22] Millard, M., Uchida, T., Seth, A., and Delp, S. L., 2013, "Flexing Computational Muscle: Modeling and Simulation of Musculotendon Dynamics," J. Biomech. Eng., **135**(2), p. 021005. https://doi.org/10.1115/1.4023390.

[23] Veerkamp, K., Van Der Krogt, M. M., Harlaar, J., O'Brien, T. D., Kalkman, B., Seth, A., and Bar-On, L., 2023, "Personalisation of Plantarflexor Musculotendon Model Parameters in Children with Cerebral Palsy," Ann. Biomed. Eng., **51**(5), pp. 938–950. https://doi.org/10.1007/s10439-022-03107-8.

[24] Luis, I., Afschrift, M., and Gutierrez-Farewik, E. M., 2024, "Experiment-Guided Tuning of Muscle–Tendon Parameters to Estimate Muscle Fiber Lengths and Passive Forces," Sci. Rep., **14**(1), p. 14652. https://doi.org/10.1038/s41598-024-65183-1.

[25] Holzbaur, K. R. S., Murray, W. M., and Delp, S. L., 2005, "A Model of the Upper Extremity for Simulating Musculoskeletal Surgery and Analyzing Neuromuscular Control," Ann. Biomed. Eng., **33**(6), pp. 829–840. https://doi.org/10.1007/s10439-005-3320-7.

[26] Saul, K. R., Hu, X., Goehler, C. M., Vidt, M. E., Daly, M., Velisar, A., and Murray, W. M., 2015, "Benchmarking of Dynamic Simulation Predictions in Two Software Platforms

Using an Upper Limb Musculoskeletal Model," Comput. Methods Biomech. Biomed. Engin., **18**(13), pp. 1445–1458. https://doi.org/10.1080/10255842.2014.916698.

[27] Melissa Daly, 2011, "Adaptations Following Upper Extremity Resistance Training in Older Adults."

[28] Delp, S. L., Anderson, F. C., Arnold, A. S., Loan, P., Habib, A., John, C. T., Guendelman, E., and Thelen, D. G., 2007, "OpenSim: Open-Source Software to Create and Analyze Dynamic Simulations of Movement," IEEE Trans. Biomed. Eng., **54**(11), pp. 1940–1950. https://doi.org/10.1109/TBME.2007.901024.

[29] McFarland, D. C., Brynildsen, A. G., and Saul, K. R., 2020, "Sensitivity of Neuromechanical Predictions to Choice of Glenohumeral Stability Modeling Approach," J. Appl. Biomech., **36**(4), pp. 249–258. https://doi.org/10.1123/jab.2019-0088.

[30] Mendias, C. L., Roche, S. M., Harning, J. A., Davis, M. E., Lynch, E. B., Sibilsky Enselman, E. R., Jacobson, J. A., Claflin, D. R., Calve, S., and Bedi, A., 2015, "Reduced Muscle Fiber Force Production and Disrupted Myofibril Architecture in Patients with Chronic Rotator Cuff Tears," J. Shoulder Elbow Surg., **24**(1), pp. 111–119. https://doi.org/10.1016/j.jse.2014.06.037.

[31] Baxter, J. R., and Hast, M. W., 2018, "Tendon Slack Length Is the Primary Determinant of Plantarflexor Muscle-Tendon Function in Computational Simulations of Gait." https://doi.org/10.1101/328435.

[32] Hawkes, D. H., Alizadehkhaiyat, O., Kemp, G. J., Fisher, A. C., Roebuck, M. M., and Frostick, S. P., 2012, "Shoulder Muscle Activation and Coordination in Patients with a Massive Rotator Cuff Tear: An Electromyographic Study," J. Orthop. Res., **30**(7), pp. 1140–1146. https://doi.org/10.1002/jor.22051.

[33] Kelly, B. T., Williams, R. J., Cordasco, F. A., Backus, S. I., Otis, J. C., Weiland, D. E., Altchek, D. W., Craig, E. V., Wickiewicz, T. L., and Warren, R. F., 2005, "Differential Patterns of Muscle Activation in Patients with Symptomatic and Asymptomatic Rotator Cuff Tears," J. Shoulder Elbow Surg., **14**(2), pp. 165–171. https://doi.org/10.1016/j.jse.2004.06.010.

[34] Pataky, J., Engle, L., Seelam, V., Khandare, S., Moore, Z. M., Armstrong, A. D., and Vidt, M. E., 2022, "Movement Compensation Is Driven by the Deltoid and Teres Minor Muscles Following Severe Rotator Cuff Tear," Clin. Biomech., **100**, p. 105799. https://doi.org/10.1016/j.clinbiomech.2022.105799.

[35] Dixit, N. N., McFarland, D. C., Fisher, M. B., Cole, J. H., and Saul, K. R., 2020, "Integrated Iterative Musculoskeletal Modeling Predicts Bone Morphology Following Brachial Plexus Birth Injury (BPBI)," J. Biomech., **103**, p. 109658. https://doi.org/10.1016/j.jbiomech.2020.109658.